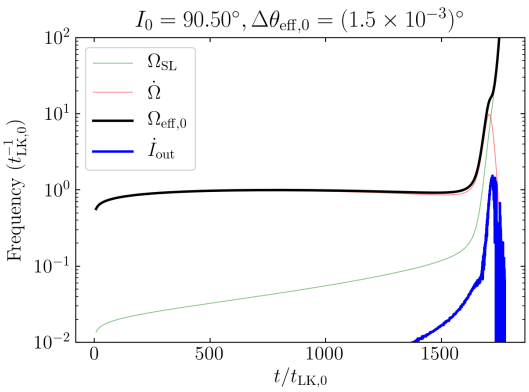

Figure 1: Plot of precession frequencies for $I_0 = 90.5°$, "slow merger". $\dot{I}_{\rm e} \equiv \left|{\rm d}\hat{\mathbf{\Omega}}_{\rm e,0}/{\rm d}t\right|$ is shown in blue.

1 Theory

As Dong correctly pointed out last week, I left out a term (and flipped a sign), and the correct equations of motion are

$$\frac{{\rm d}\theta}{{\rm d}t} = -\dot{I}_{\rm e}\cos\phi, \tag{1}$$

$$\frac{{\rm d}\phi}{{\rm d}t} = \Omega_{\rm e} + \dot{I}_{\rm e}\cot\theta\sin\phi. \tag{2}$$

This system of equations is useful because $\dot{I}_{\rm e}$ obeys the following ODE (note that I is the LK-averaged I and turns out to be very nearly constant, so its derivative is dropped):

$$-\dot{\Omega}\sin I_{\rm e} + \Omega_{SL}\sin(I+I_{\rm e}) = 0, \tag{3}$$

$$\dot{I}_{\rm e}\left(-\dot{\Omega}\cos I_{\rm e} + \Omega_{\rm SL}\cos(I+I_{\rm e})\right) = \ddot{\Omega}\sin I_{\rm e} - \dot{\Omega}_{\rm SL}\sin(I+I_{\rm e}), \tag{4}$$

$$= \ddot{\Omega}\frac{\Omega_{\rm SL}\sin(I+I_{\rm e})}{\dot{\Omega}} - \dot{\Omega}_{\rm SL}\sin(I+I_{\rm e}), \tag{5}$$

$$\dot{I}_{\rm e}(-\cot I_{\rm e} + \cot(I+I_{\rm e})) = \frac{\rm d}{{\rm d}t}\left(\ln\left(-\dot{\Omega}\right) - \ln\Omega_{\rm SL}\right). \tag{6}$$

The coefficient of $\dot{I}_{\rm e}$ is almost always very large except when $\pi - I_{\rm e} \approx I + I_{\rm e}$, where it is ~ -2 (negative when $I > 90°$), and $-\dot{\Omega} \simeq \Omega_{\rm SL}$. Thus, we find

$$\max\dot{I}_{\rm e} \simeq \frac{1}{2}\frac{\rm d}{{\rm d}t}\left(\frac{\Omega_{\rm SL}}{-\dot{\Omega}}\right) \equiv \frac{1}{2}\left(\dot{\mathscr{A}}\right)_{\mathscr{A}=1}. \tag{7}$$

Here, $\mathscr{A} \equiv \Omega_{\rm SL}/(-\dot{\Omega})$ is the adiabaticity parameter from LL18. We omit the subscript going forwards.

Furthermore, since $\dot{I}_{\rm e}$ must integrate to $\min(I, \pi/2 - I)$, this provides a constraint on the width of $\dot{I}_{\rm e}(t)$, and we can write down

$$\dot{I}_{\rm e} \simeq \frac{\dot{\mathscr{A}}}{2}\exp\left[-\frac{t^2}{(2I/\dot{\mathscr{A}})^2/\pi}\right] \tag{8}$$

As can be seen in the figure shown in the previous writeup, $\dot{I}_{\rm e}$ is indeed peaked, though somewhat asymmetric (Fig. 1). If we drop the $\dot{I}_{\rm e}$ contribution in Eq. (2) and assume $\Omega_{\rm e}$ is approximately con-

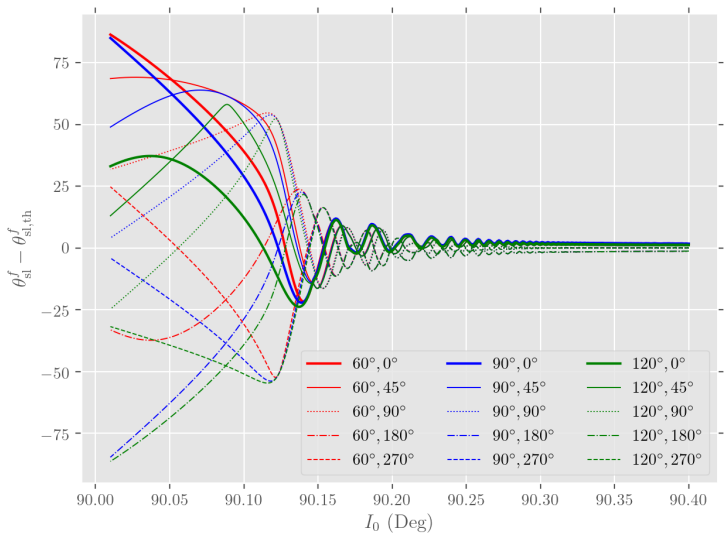

Figure 2: Old plot of the difference between the final spin orbit misalignment angle and the predicted one, as a function of inclination I_0. Legend labels are $(\theta^i_{\rm sl}, \phi^i_{\rm sb})$; the weird coordinates are an artifact of being an old plot, but the dependence on $\phi^i_{\rm sb} \approx \phi^i_{\rm e}$ and not on $\theta^i_{\rm sl} \approx I - \theta^i_{\rm e}$ is clear.

stant, the integral that determines $\Delta\theta_{\rm e}$ is then

$$\Delta\theta_{\rm e} = \int_{-\infty}^{\infty} -\dot{I}_{\rm e} e^{i(\phi_0 + \Omega_{\rm e} t)}\, {\rm d}t, \tag{9}$$

$$= -I e^{i\phi_0} \exp\left[-\frac{\Omega_{\rm e}^2 I^2}{\pi \dot{\mathscr{A}}^2}\right]. \tag{10}$$

Note the dependence on $\phi_0 = \phi_{\rm sb,0}$ and the lack of dependence on $\theta_{\rm sb,0}$: this are both results that agree with simulations (see e.g. Fig. 2).

Caveats:

- Of course, a treatment with non-constant $\Omega_{\rm e}$ is possible, and a first order correction $\phi = \phi_0 + \Omega_{\rm e} t + \dot{\Omega}_{\rm e} t^2/2$ simply changes the width of the Gaussian a bit.
- The approximation of dropping $\dot{I}_{\rm e}$ in Eq. (2) is less legal. However, if ϕ is fast-varying (requiring $\Omega_{\rm e} \geq \dot{I}_{\rm e}$), then dropping $\dot{I}_{\rm e}$ should be a very good approximation, as $\sin\phi$ should significantly suppress the contribution. The $\cot\theta$ enhancement however illustrates that, regardless of how much $\Omega_{\rm e} \gg \dot{I}_{\rm e}$, there will always be some IC for which $\theta_{\rm e}$ can evolve significantly.

2 Comparison to Simulations

This section is incomplete, I plan to finish it tomorrow morning (numerically exploring the effective quantities I defined above). I will at least discuss the three plots below.

In Fig. 3, we display a histogram of the $\Delta\theta_{\rm e}$ values, each for an isotropically sampled initial spin condition. Alternatively, we can numerically compute the integral

$$\Delta\theta_{\rm guess}(\phi^i_{\rm e}) = \int_0^{t_{\rm f}} -\dot{I}_{\rm e} \cos\left(\Omega_{\rm e} t + \phi^i_{\rm e}\right)\, {\rm d}t, \tag{11}$$

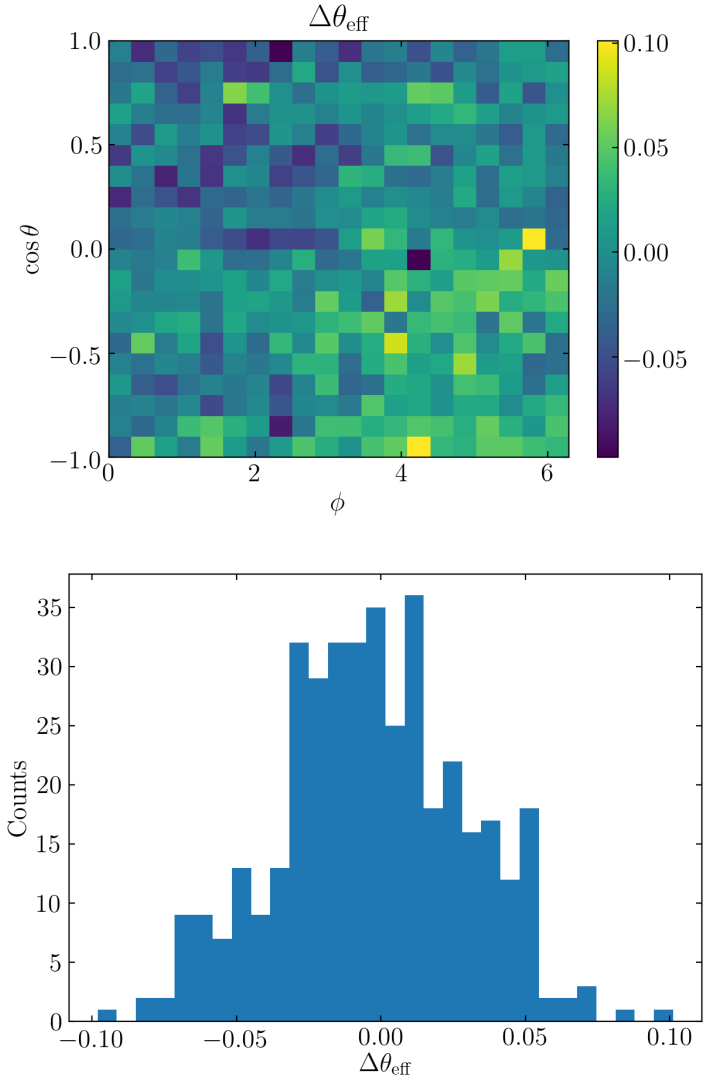

Figure 3: Top: Plot of the deviations $\Delta\theta_{\text{e}}$ as a function of initial spin vector orientation, θ_{e} and ϕ_{e}. This plot is corrected from last week. Two notable outliers were found, though they've been omitted from the colorbar for clarity (shown later). The distribution of the 400 values is shown in the bottom panel.

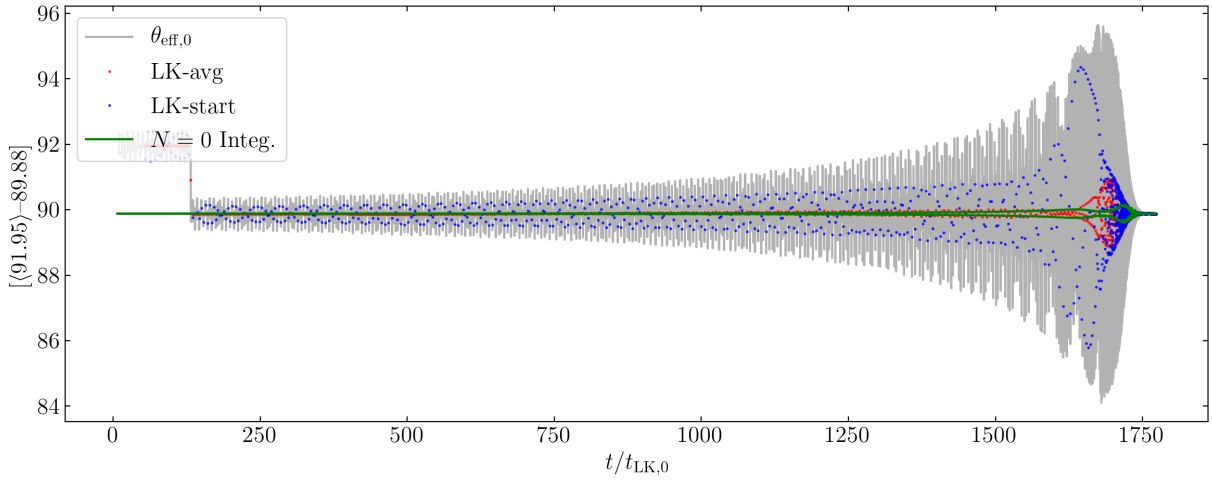

Figure 4: Possible resonant case similar to that observed in LL17, but using the parameters from the Paper II regime. The total $\Delta\theta_{\rm e}$ is 2°, owing to an instantaneous kick at around $t = 125$. I intend to investigate this further next week, but the behavior is similar to that seen in LL17.

and take the maximum over a few choices of $\phi_{\rm e}$. This does not require any spin evolutions, only the orbital evolution, and should provide an upper bound on the maximum $\Delta\theta_{\rm e}$ observed. Indeed, this procedure estimates $\max \Delta\theta_{\rm e} \approx 0.09$, very consistent with the histogram, but *failing* to capture the outlier in Fig. 4. This suggests that the EOM written down for $\dot{\theta}_{\rm e}$ is correct, though it does not validate the analysis of the previous section.